High spatial resolution 2C-2D PIV measurements using a 47 MPx sensor of high Reynolds number turbulent boundary layer flow

Bihai Sun[1,*], Muhammad Shehzad[1], Chris Willert[2], Jean-Marc Foucaut[3], Christophe Cuvier[3] and Yasar Ostovan[3], Callum Atkinson[1], Julio Soria[1]

1: 1: Laboratory for Turbulence Research in Aerospace & Combustion (LTRAC), Department of Mechanical and Aerospace Engineering, Monash University (Clayton Campus), VIC 3800, Australia
2: German Aerospace Center (DLR), Institute of Propulsion Technology, Köln, Germany
3: Univ. Lille, CNRS, ONERA, Arts et Métiers Institute of Technology, Centrale Lille, UMR 9014 - LMFL - Laboratoire de Mécanique des Fluides de Lille (LMFL) - Kampé de Fériet, F-59000, Lille, France
*Corresponding author: bihai.sun@monash.edu

Keywords: 2C-2D PIV, lens distortion, turbulent boundary layer

ABSTRACT

In the past decade, advances in electronics technology have made larger imaging sensors available to the experimental fluid mechanics community. These advancements have enabled the measurement of 2-component 2-dimensional (2C-2D) velocity fields using particle image velocimetry (PIV) with much higher spatial resolution than previously possible using a single camera. Although previously reported experiments have incorporated multiple-camera array to acquire high spatial resolution PIV, using a single large camera can greatly reduce the complexity of the experimental setup as well as the error introduced by the calibration between the cameras. In this paper, the ability of a single large sensor for high spatial resolution PIV is demonstrated by performing the measurement of a zero-pressure-gradient turbulent boundary layer (ZPG-TBL). In post-processing the PIV images, the lens distortion error is of particular importance, as the lens distortion error increases with the size of the imaging sensor. The third-order polynomial functions are used to model the lens distortion in this study, and the correction is performed on the PIV vectors to save computational cost. The first- and second-order statistics are calculated and compared with the profiles captured by small camera arrays, and the result shows that the corrected profiles agree well with the previously acquired data, therefore, the lens distortion error can be corrected.

1. Introduction

Turbulent boundary layer (TBL) flows in both zero pressure gradient (ZPG) and adverse pressure gradient (APG) environments are ubiquitous throughout the industry, transport, energy generation and environmental flows. Although TBL flows have been investigated for more than a century, we are still lacking a pertinent understanding of their detailed structure, and in some environments such as APG, we do not even have a unifying scaling for these flows. This is partly

due to the lack of comprehensive experimental data at a sufficiently high Reynolds number. Very often, the facilities are too small to reach high Reynolds numbers and to let the boundary layer develop sufficiently enough to reach some state of equilibrium where theoretical approaches can be relevant. Moreover, measurements are generally quite limited in the spatial resolution, leading to a lack of detailed characterisation of the flow itself but also of the boundary conditions, which makes the data very difficult to use in practice, both for physical understanding and for models validation.

An extensive 2C-2D large field-of-view PIV and 3C-2D stereo PIV experiment campaign of a zero-, favourable- and adverse-pressure gradient high Reynolds number turbulent boundary layer flow undertaken in the LMFL High Reynolds Number Boundary Layer Wind Tunnel reported by Cuvier et al. (2017) explored several extreme cases of high-resolution PIV. The time-resolved transfer-bandwidth-limited high-spatial-resolution PIV, also incorporated by Willert et al. (2018) achieved high resolution in both spatial domain in the wall-normal direction, which is 504 vectors over a 0.025 m field of view, and in temporal domain, which is up to 6,667 Hz. However, in this set-up, the streamwise field of view is very limited, therefore, the flow structures in the turbulent wall-bounded flow can not be captured and studied. On the other size, another set-up in the experimental campaign consists of 16 cameras in the streamwise directions to achieve a field of view of 3.466 m in the streamwise direction and 0.255 m in the wall-normal direction, with a vector field size of 3,250 $\times$ 238. The experiment reported in this paper is complementary to the experiments described above in the same facility. Using a single 47 MPixel camera, the spatial resolution in the wall-normal direction can be doubled, and in the streamwise direction this camera has a field of view equivalent to 2.5 cameras in the experimental set-up reported by Cuvier et al. (2017). Therefore, the experimental set-up can be greatly simplified with less potential error source from the calibration between cameras.

The processing of the PIV images taken by the high-spatial-resolution camera highlighted the measurement error caused by the lens distortion. The distribution and size of the error introduced by lens distortion were modelled using third-order polynomial functions. This analysis found that the bias PIV error produced by the local lens distortion within an interrogation window is comparable to or below the uncertainty of a typical PIV measurement and, therefore, indistinguishable from the experimental uncertainty of 2C-2D PIV. This result suggests a simplified and more computationally efficient correction approach to 2C-2D PIV using large sensors affected by lens distortion.

2. HSR PIV Measurements of high Reynolds number ZPG-TBL

The HSR 2C-2D PIV experiments were carried out in the High Reynolds Number Boundary Layer Wind Tunnel of the Laboratoire de Mécanique des Fluides de Lille (LMFL). This wind tunnel has a streamwise test section length of $20.6m$, and a cross-sectional area of $2m$ wide by $1m$ high. The facility is constructed using a metal frame with high quality $10mm$ thick glass walls along the entire test section providing complete optical access throughout its test section. This wind tunnel

test section has a custom-designed floor-mounted model, as shown in Fig. 1 to generate a high Reynolds number turbulent boundary layer in an adverse pressure gradient environment over a relatively large streamwise extend. However, this experiment is performed $6.8m$ downstream of the tripping location of the turbulent boundary layer, which is upstream of the model and corresponds to station B in Fig. 1. The free-stream flow velocity for the experiment was set to $U_\infty = 9m/s$ at the inlet of the test section with the ZPG-TBL at the measurement location having a Reynolds number based on the momentum thickness, $Re_\theta = 8,120$, a boundary layer thickness defined by the location where the mean velocity reaches 99% of the free-stream velocity of $\delta \approx 103mm$ and a viscous length $l^+ \approx 40\mu m$.

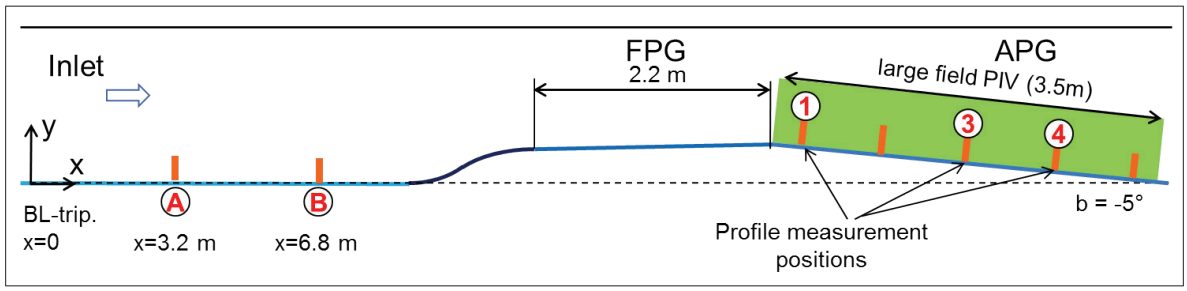

Figure 1. Side view of wind tunnel test section with APG-Model and measurement positions.

The single-exposed PIV images were acquired using an Imprex Tiger T8810 CCD camera with 47 megapixel array and a dynamic range of 12 bits. The camera's sensor has a pixel array of $8,864 \times 5,288$ with a pixel size of $5.5\mu m$, resulting in a $48.7mm \times 29.0mm$ ($56.7mm$ diagonal) array. The synchronisation between the pulses of the Nd:YAG laser and the camera is the same as used in previous PIV experiments in the same facility Cuvier et al. (2017). In the presented experiments, a telephoto lens (Hasselblad Zeiss Sonnar 250mm f/5.6) with a $45mm$ extension tube was used. This camera lens combination was used to image the near-wall region of the high Reynolds number ZPG-TBL at a large magnification of $M = 0.19$, corresponding to a pixel size of $28.9\mu m$ in object space, resulting in a measurement area of $2.46\delta \times 1.45\delta$. The imaging set-up is shown in figure 2. The single-exposed PIV image pairs were processed using an in-house multigrid/multipass 2C-2D cross-correlation digital PIV analysis algorithm (Soria, 1996).

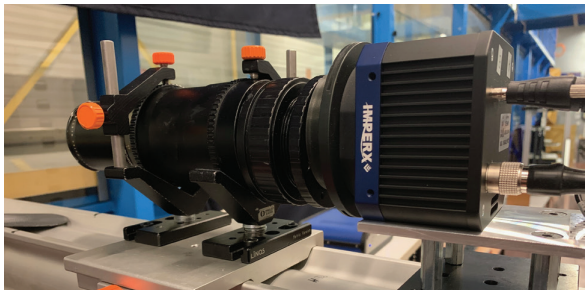

Figure 2. Imaging setup for the present experiment including a 47 MPixel CCD camera and a 250mm-focal-length telephoto lens with extension tube.

In this study, the streamwise, wall-normal and spanwise directions of the ZPG-TBL are denoted by x, y and z respectively, with the respective velocity components denoted by u, v and w. The mean velocities in the x, y and z are denoted by U, V and W respectively, while the corresponding fluctuating velocities are denoted by u', v' and w'. An overbar $\overline{\square}$ represents the ensemble average of the variables encompassed by it. The PIV acquisition parameters are summarized in table 1.

Since the severity of lens distortion typically increases monotonically from the centre of the lens towards its edge, large sensors are more prone to lens distortions therefore, it must be corrected. The PIV raw images in this experiment are corrected using the method described by Sun et al. (2021). In the distortion correction process of the PIV images, a third-order polynomial distortion model is used, and the correction is performed by moving PIV velocity vectors to the correct position rather than dewarp the images to reduce computational cost.

Table 1. The PIV acquisition parameters for ZPG-TBL measurements

Property	Symbol	Units	Value
Free stream velocity	U_∞	ms^{-1}	9.64
Friction Reynolds number	Re_τ		2,386
Friction velocity	u_τ	ms^{-1}	0.348
Number of samples	N		34,535
Field of View	FOV	mm	255 × 152
	FOV	δ	2.46 × 1.45
PIV final window size	IW_x	$pixel$	32
in streamwise direction	IW_x	μm	927
	IW_x^+	l^+	21.7
PIV final window size	IW_y	$pixel$	8
in wall-normal direction	IW_y	μm	232
	IW_y^+	l^+	5.42
PIV measurement volume	IW_z	μm	400
in spanwise direction	IW_z^+	l^+	4.68
Uncertainty in mean velocity	ϵ_U		0.825%
Uncertainty in the Reynolds normal stresses	$\epsilon_{\overline{u'u'}}$, $\epsilon_{\overline{v'v'}}$		0.381%
Uncertainty in the Reynolds shear stress	$\epsilon_{\overline{u'v'}}$		0.695%

Table 2. Turbulent boundary layer characteristics compared with EuHIT experiment (Cuvier et al., 2017)

	U_∞ (m/s)	δ_{99} (mm)	u_τ (m/s)	Re_τ
Current experiment	9.64	103	0.348	2,386
EuHIT	9.64	104	0.346	2,360

3. Results

The first- and second-order statistics of the velocity field of the ZPG-TBL are presented and compared with those measured in the same facility under similar flow conditions in a previous experimental campaign (EuHIT experiment) (Cuvier et al., 2017), as well as first- and second-order statistics of the velocity field of a ZPG-TBL DNS with $Re_\theta = 6,500$ (Sillero et al., 2014). The PIV data provided from the EuHIT database was processed using an interrogation window size of $20^+ \times 5^+$ in the streamwise and wall-normal directions for $y < 5mm$ with the superscript $^+$ denoting viscous units. Thus, the spatial resolution is similar to the data presented in this paper. However, since the sensor used in the EuHIT measurement is only 35% of the size of the sensor used in the presented study, the lens distortion in the EuHIT data set is minimal, since assuming lens distortion to be the same for both experiments, the estimated error introduced by lens distortion is about 0.2%. For $y > 5mm$ the velocity fields were measured using SPIV, which includes corrections for any image distortion through the SPIV image calibration process. So, the first- and second-order statistics profiles provided from the EuHIT experiment can be deemed to be image distortion-free. Also, note that SPIV data from EuHIT experiment has a lower spatial resolution than the near-wall 2C-2D PIV. Therefore, in the presented experiment, one single camera covers the wall-normal domain that is previously measured by two cameras, with high spatial resolution and a larger streamwise field of view.

The boundary layer characteristics calculated from the mean profile based on dewarped 2C-2D PIV analysis presented in table 2 compare favourably with the boundary layer statistics measured in the EuHIT experiment. The mean streamwise velocity profiles are given and compared in figure 3. These results show that, in the wall region, the mean streamwise velocity profile measured based on the raw distorted images deviates from the EuHIT profile with a maximum difference of as much as 80%, clearly illustrating that lens distortion leads to significant errors in these measurements and must be corrected. The maximum deviation of the profile is near the wall, which is near the edge of the image where lens distortion is a maximum. However, the figure shows that most of the error from the lens distortion can be corrected, and the corrected mean velocity profile agrees well with the EuHIT dataset.

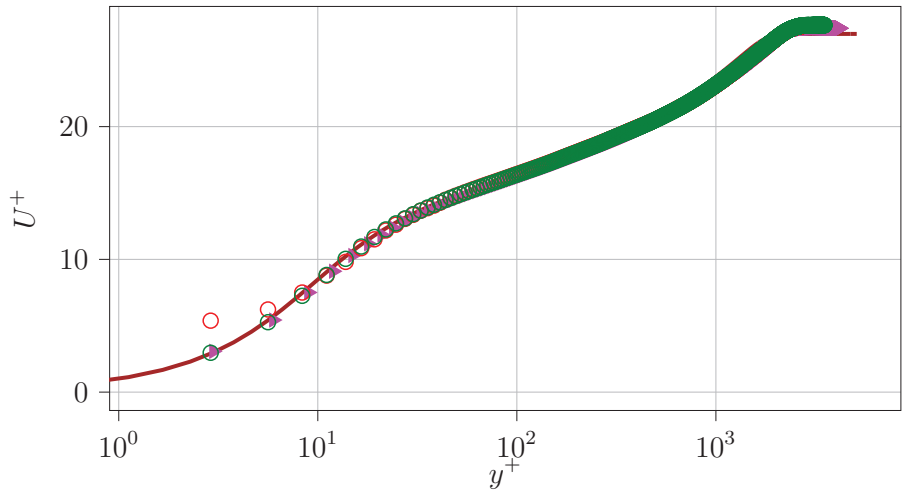

Figure 3. Mean streamwise velocity profile in wall units. The profile is compared with an experimental data taken in similar flow conditions (Cuvier et al., 2017) (EuHIT) as well as DNS simulation with $Re_\theta = 6500$ (Sillero et al., 2014) —: DNS. ◀: EuHIT. ○: Distorted. ○: Corrected for distorsion.

The measured Reynolds stress profiles are presented in figure 4 and compared with the profiles from the EuHIT experiment as well as the highly resolved DNS data. These results show that dewarping does not affect the $\overline{u'v'}^+$ and $\overline{v'v'}^+$ profiles as much as the $\overline{u'u'}^+$ profile. However, the profiles based on the raw distorted PIV images are slightly lower than the profiles based on the dewarped PIV images. The $\overline{u'u'}^+$ profile based on the raw PIV images is up to 12% lower than the profile from the EuHIT experiment with the peak slightly shifted to a higher y^+ value. Again, most of the errors in the Reynolds stress can be corrected.

4. Concluting remarks

This paper presents a 2C-2D PIV experiment performed on ZPG TBL using a single 47 MPixel camera. It demonstrates that a single high spatial resolution camera can substitute multiple cameras for high spatial resolution PIV to avoid complex experimental setup and calibration process. However, the lens distortion can introduce considerable error when a large-size imaging sensor is used and must be corrected for. In the reported experiment, third-order polynomial functions distortion model is used to correct the lens distortion and the correction is performed on the PIV vectors instead of images to save computational power. The result shows that most of the distortions in the PIV images are corrected, and the first and second-order statistics agree well with the previous PIV measurements with multiple cameras.

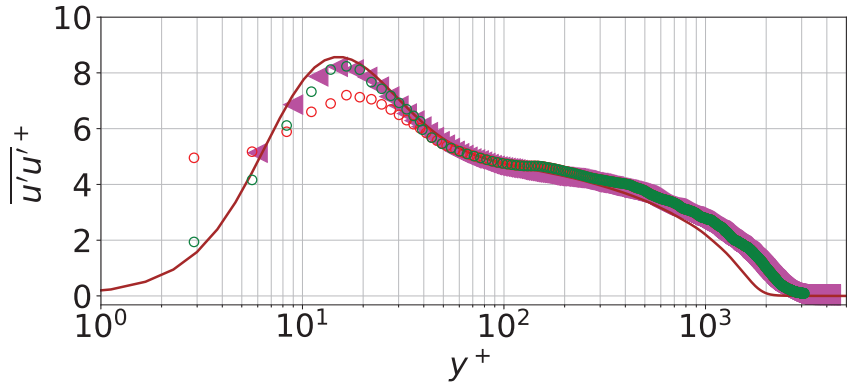

(a)

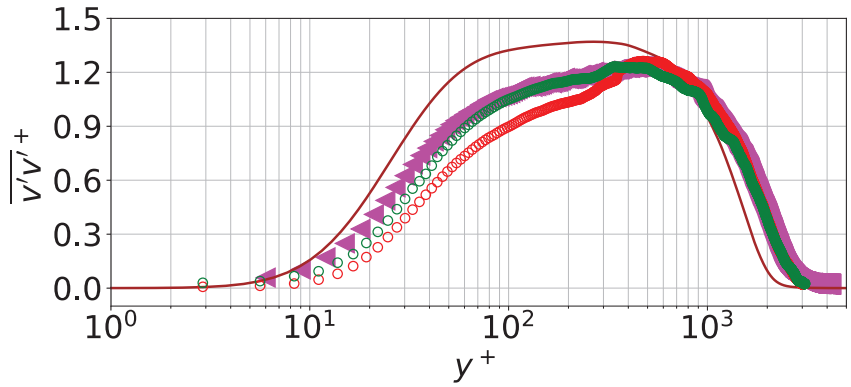

(b)

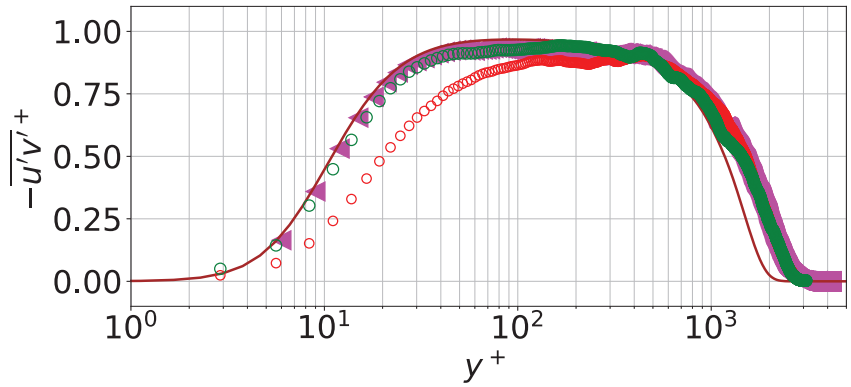

(c)

Figure 4. (a) Streamwise Reynolds stress profile ($\overline{u'u'}^+$), (b) wall-normal Reynolds stress profile ($\overline{v'v'}^+$) and (c) Reynolds shear stress profile ($-\overline{u'v'}^+$) The profiles are compared with experimental data taken under similar flow conditions (EuHIT Experiment) (Cuvier et al., 2017), as well as a DNS simulation with $Re_\theta = 6500$ (Sillero et al., 2014) —: DNS. ◂: EuHIT. ○: Distorted. ○: Corrected for lens distortion.

References

Cuvier, C., Srinath, S., Stanislas, M., Foucaut, J. M., Laval, J. P., Kaehler, C. J., ... Soria, J. (2017). Extensive characterisation of a high reynolds number decelerating boundary layer using advanced optical metrology. *Journal of Turbulence*, *18*(10), 929-972. Retrieved from https://doi.org/10.1080/14685248.2017.1342827 doi: 10.1080/14685248.2017.1342827

Cuvier, C., Srinath, S., Stanislas, M., Foucaut, J. M., Laval, J. P., Kähler, C. J., ... Soria, J. (2017). Extensive characterisation of a high reynolds number decelerating boundary layer using advanced optical metrology. *Journal of Turbulence*, *18*(10), 929-972. doi: 10.1080/14685248.2017.1342827

Sillero, J. A., Jiménez, J., & Moser, R. D. (2014). Two-point statistics for turbulent boundary layers and channels at reynolds numbers up to $\delta+ \approx 2000$. *Physics of Fluids*, *26*(10), 105-109. doi: 10.1063/1.4899259

Soria, J. (1996). An investigation of the near wake of a circular cylinder using a video-based digital cross-correlation particle image velocimetry technique. *Experimental Thermal and Fluid Science*, *12*(2), 221–233. doi: 10.1016/0894-1777(95)00086-0

Sun, B., Shehzad, M., Jovic, D., Cuvier, C., Willert, C., Ostovan, Y., ... Soria, J. (2021, 9). Distortion correction of two-component two-dimensional piv using a large imaging sensor with application to measurements of a turbulent boundary layer flow at $\mathrm{Re}_\tau = 2386$. *Experiments in Fluids*, *62*, 183. Retrieved from https://link.springer.com/10.1007/s00348-021-03273-w doi: 10.1007/s00348-021-03273-w

Willert, C., Cuvier, C., Foucaut, J., Klinner, J., Stanislas, M., Laval, J., ... Roese, A. (2018, 2). Experimental evidence of near-wall reverse flow events in a zero pressure gradient turbulent boundary layer. *Experimental Thermal and Fluid Science*, *91*, 320–328. doi: 10.1016/j.expthermflusci.2017.10.033